Sensors and Materials, Vol. 34, No. 12 (2022) 4669–4686
MYU Tokyo

S & M 3136

Wildfire Impact on Cerro Cora National Park Measured Using Landsat and Sentinel Images

Jisung Kim,[1*] Joonseok Oh,[2**] and Jaeyong Yoo[2]

[1]Civil and Environmental System Engineering, Sungkyunkwan University,
2066 Seobu-ro, Jangan-gu, Suwon-si, Gyeonggi-do 16419, Republic of Korea
[2]Land & Geo-spatial Consulting Group, Geomexsoft., Ltd.,
#103-306, 67 Seobinggo-ro, Yongsan-gu, Seoul 04385, Republic of Korea

(Received April 26, 2022; accepted August 3, 2022)

Keywords: NBR, NDVI, tasseled cap transformation, wildfire damaged area, wildfire impact

To prepare for and recover from damage due to wildfires, it is necessary to investigate and analyze the impacts of wildfires. To date, various wildfire research methodologies have been conducted and analyzed. The impact of fire tends to be difficult to generalize because it is closely related to many factors, such as the characteristics of the area and the seasonal distribution of vegetation. Therefore, it is necessary to conduct case studies considering the geographical, vegetational, and seasonal characteristics of the area for impact estimation. Quantitative and qualitative analyses of the wildfire that occurred in Cerro Cora National Park, Paraguay in August 2021 are needed to recover from the damage and to prepare for future wildfires. Therefore, in this study, we analyzed the impact of the wildfire in Cerro Cora National Park. To calculate the damaged area and severity, the normalized burn ratio and normalized difference vegetation index obtained from Landsat and Sentinel images were used. The tasseled cap transformation was also used to investigate the characteristic variation. To calibrate the seasonal factor, long-term analysis was performed, and short-term analysis was performed to determine the immediate impact of the wildfire. As a result, the damaged area, severity, and restoration for each area were estimated. In addition, characteristic variations of the area were identified. Furthermore, the reliability of the study was enhanced by comparing the results from each satellite image and index.

1. Introduction

In August 2021, a wildfire in Cerro Cora National Park, which is one of the national parks in Paraguay, damaged forest resources. Data on the damage caused by forest fire and changes in land characteristics are needed to identify vegetation, restore the forest, and prepare for future wildfires. However, as the area is vast, it is difficult to conduct on-site investigations to identify the extent of damage, and it is difficult to measure the amount of damage and changes in land characteristics because forest resources were not identified previously.

*Corresponding author: e-mail: jskim6687@skku.edu
**Corresponding author: e-mail: joon@geomexsoft.co.kr
https://doi.org/10.18494/SAM3953

ISSN 0914-4935
https://myukk.org/

These difficulties can be overcome using remote sensing. In particular, because satellite imagery can reveal a wide range of information about difficult-to-access areas, it is easy to understand wildfire damage and changes in land characteristics,[1] as proven by various recent research cases. Collins *et al.* applied artificial intelligence to measure fire severity using Landsat and the random forest algorithm, and studied the learning data.[2] The Landsat image was found to be effective in measuring fire severity. In contrast, Seydi *et al.* used Sentinel and Moderate Resolution Imaging Spectrometer (MODIS) to evaluate forest fire damage and verified their effectiveness of fire by comparing the results with Landsat measurements.[3] It was found that damage due to forest fire can be quantified using satellite images from Landsat, Sentinel, and MODIS. In addition, studies have been conducted recently to confirm forest fire damage using Korean Multi-Purpose Satellite (KOMPSAT) images in addition to other satellite images.[4,5]

Most of these studies used the vegetation index, which is an effective factor to evaluate the damage due to forest fire. Representative indices for estimating forest fire damage are the normalized difference vegetation index (NDVI) and normalized burn ratio (NBR). NDVI is used to indicate the vegetation distribution and activity, as well as chlorophyll content.[6] Because forest fire affects both vegetation activity and chlorophyll, the amount of damage can be calculated using NDVI. Therefore, research on using NDVI to measure forest fire damage is ongoing.[7–14] Similarly, there are many studies using NBR.[2–5,9,10,13,15–19] NBR uses the difference between the near-infrared (NIR) and short-wave infrared (SWIR) spectra as an index to measure fire severity. NBR can be used to determine the extent of damage caused by wildfires, as well as the recovery from such damage.

However, in addition to the vegetation index, there is tasseled cap transformation as one of the methods to understand the land characteristics.[20–27] The tasseled cap transformation can help analyze the structure of multiband sensor data and reduce the amounts of data. In addition, it is used as a technical and analytical tool in various areas of ecological research as a traditional image conversion method to monitor surface and environmental changes.[20] There are many cases where the tasseled cap transformation was used to determine the amounts of damage and recovery caused by wildfires.[9,28,29] The transformation has its own merits to provide a mechanism for data volume reduction and enhanced data interpretability by emphasizing the structures in the spectral data, which arise as a result of particular physical characteristics of scene classes.[20]

From the above studies, it is possible to derive the vegetation status and land characteristics using the vegetation index and tasseled cap. However, because the above studies depend on the site characteristics, different results may be obtained depending on the location and geographical characteristics. In particular, there are few previous studies about the wildfires in Cerro Cora National Park; thus, there is a limited understanding of the amount of damage and land characteristics caused by those wildfires. It is necessary to improve the existing research methodology to estimate the impacts of wildfires in Cerro Cora National Park.

To address this limitation, not only should the vegetation index and tasseled cap be utilized to understand the vegetation change and land characteristics, but various perspectives through images acquired at multiple times should also be considered. Therefore, in this study, the amount of damage and changes in land characteristics due to the wildfire in Cerro Cora National Park are estimated.

2. Materials and Methods

2.1 Methods

This study comprises period setting, image acquisition, transformation, and analysis steps. In the period setting, appropriate image acquisition dates are determined to observe the damage and changes in land characteristics caused by forest fire. In the image acquisition step, images are acquired by time period, satellite type, and band for analysis. In the transformation step, NDVI, NBR, and the tasseled cap transformation are determined from the images collected in each spatial and spectral domain, and the results are processed into data that can identify the damage and changes in land characteristics. Finally, in the analysis step, the data are analyzed by section and time (see Fig. 1).

2.1.1 Multi-temporal analysis

To understand the damage and land characteristics due to wildfires, images should be analyzed over multiple periods. The wildfires have short-, medium-, and long-term impacts, ranging from a few days to months or longer. To understand the short-term effects of wildfires, seasonal trends and changes over time should be considered through long-term analysis. After considering the seasonal and long-term effects, short-term analysis is performed to determine the impacts of forest fire. It has been proven in various studies that vegetation indices change periodically with seasons.[24,30] Therefore, both short- and long-term analyses should consider seasonal changes in vegetation. In this study, seasonal changes are considered using the results of previous studies and data from areas where vegetation changes did not occur. Figure 2 shows the multi-temporal analysis, including short- and long-term analyses, used in this study.

Long-term analysis is achieved by reviewing vegetation trends over long-term data to understand the long-term damage and forest restoration from fire. The accuracy of short-term analysis can be improved by comparing the short period from August 2021 to March 2022 with long-term historical data, such as data from the previous two years. The data used for long-term analysis are from around August 15th and around February 15th of each year. Whenever possible, the data taken at the same time of the year are used to minimize seasonal errors.

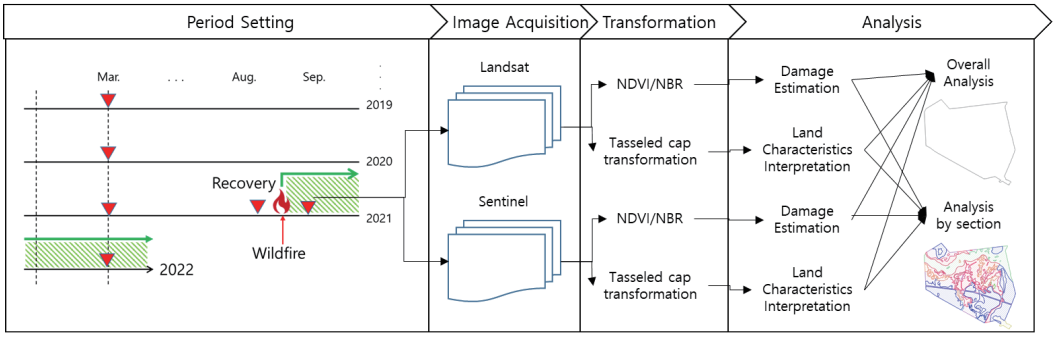

Fig. 1. (Color online) Methodology used in this study.

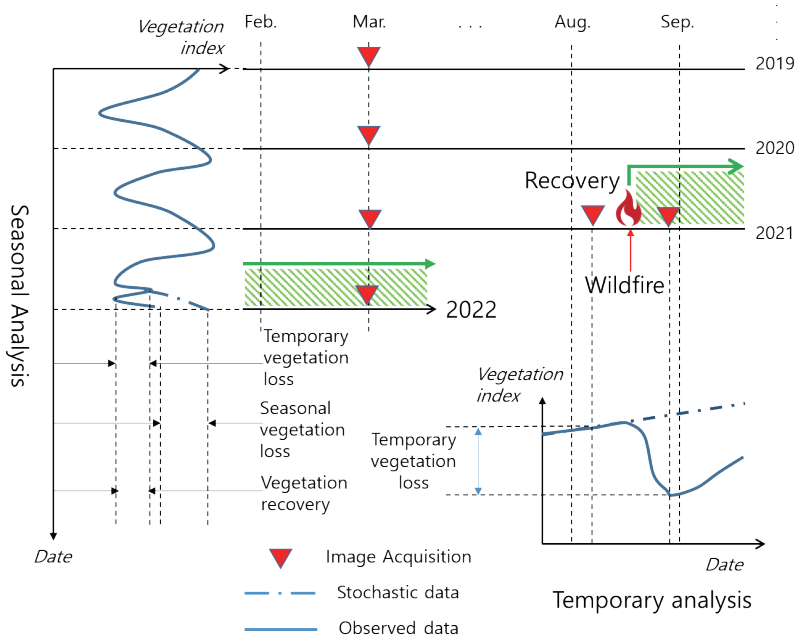

Fig. 2. (Color online) Multi-temporal analysis.

In short-term analysis, the images obtained just before the outbreak of fire and immediately after the fire has been extinguished are compared. The purpose of this study is to estimate the vegetation loss and changes in land characteristics before and after the fire to estimate the area and severity of damage due to the fire. As shown in Figs. 1 and 2, the vegetation index and characteristics are compared using two pairs of images. The amount of vegetation loss and the area of damage are calculated on the basis of the change in vegetation index. In addition, through the data obtained through the tasseled cap transformation, the characteristic changes of the entire region and each section can be analyzed.

2.1.2 Vegetation index and tasseled cap transformation

The vegetation indicators used in this study are NDVI and NBR, and the tasseled cap transformation is used to analyze the land characteristics. Table 1 shows the NDVI and NBR formulas used. Unlike the vegetation index, the tasseled cap parameter is set differently depending on the type of satellite image.

Periodic resolution according to multi-temporal analysis, spectral resolution for vegetation index and tasseled cap conversion, and spatial resolution for precision should be considered. In addition, the price of satellite imagery should be considered for the reproduction and utilization of this research. When all these factors are considered, the satellite images that meet the purpose and means of this study are Landsat and Sentinel images. More specifically, Landsat-8,9 and Sentinel-2 images are appropriate, and the corresponding tasseled cap transformation parameters are used. Each parameter is obtained from previous studies. Tables 2 and 3 show the tasseled cap parameters for Landsat-8,9 and Sentinel-2 images, respectively.

Table 1
Vegetation indices used in this study.

	Equation	Reference
NDVI	$\frac{NIR - red}{NIR + red}$	(1)
NBR	$\frac{NIR - SWIR}{NIR + SWIR}$	(10)

NIR is near-infrared band; SWIR is short-wave infrared band.

Table 2
Tasseled cap parameters for Landsat-8,9 images.[3]

	(Blue) Band 2	(Green) Band 3	(Red) Band 4	(NIR) Band 5	(SWIR1) Band 6	(SWIR2) Band 7
Brightness	0.3029	0.2786	0.4733	0.5599	0.5080	0.1872
Greenness	−0.2941	−0.2430	−0.5424	0.7276	0.0713	−0.1608
Wetness	0.1511	0.1973	0.3283	0.3407	−0.7117	−0.4599

Table 3
Tasseled cap parameters for Sentinel-2 images.[27]

	Coastal	Blue	Green	Red	RE-1	RE-2	RE-3
Brightness	0.2381	0.256	0.2934	0.3020	0.3099	0.3740	0.4180
Greenness	−0.2266	−0.2818	−0.3020	−0.4283	−0.2959	0.1602	0.3127
Wetness	0.1825	0.1763	0.1615	0.0486	0.0170	0.0223	0.0219
	NIR-1	NIR-2	WV	Cirrus	MIR-1	MIR-2	
Brightness	0.3580	0.3834	0.0103	0.0020	0.0896	0.0780	
Greenness	0.3138	0.4261	0.1454	−0.0017	−0.1341	−0.2538	
Wetness	−0.0755	−0.0910	−0.1369	0.0003	−0.7701	−0.5293	

RE, NIR, WV, and MIR stand for red edge, near infrared, water vapor, and middle infrared, respectively.

2.2 Materials

2.2.1 Image acquisition

The image acquisition time for multi-temporal analysis was determined considering seasonal changes in vegetation and the wildfire. In previous studies,[24,30] images are acquired on August 15th and February 15th of each year. In this work, the images obtained close to August 15th and February 15th were used when possible, and images within a month were used when necessary owing to weather conditions. Figure 3 shows the acquisition time of the images used in this study. For the implementation of this study, 12 Landsat images and 11 Sentinel images were used.

2.2.2 Cerro Cora National Park

The testbed of this study is Cerro Cora National Park in Paraguay. The testbed for multi-temporal studies should be a place where images can be acquired not only immediately before

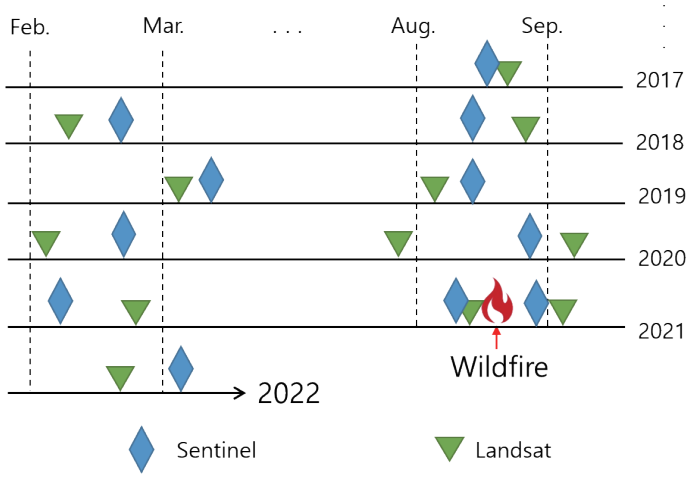

Fig. 3. (Color online) Acquisition period of Sentinel and Landsat images.

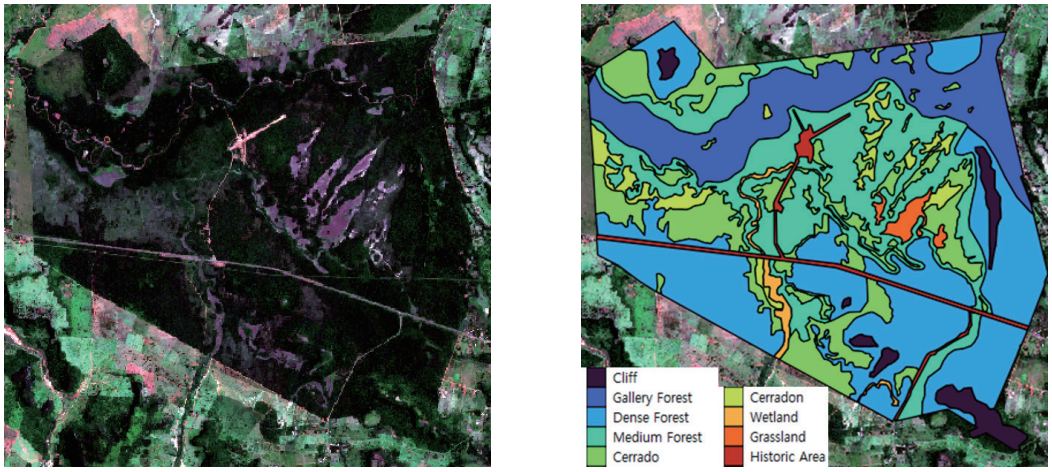

(a) (b)

Fig. 4. (Color online) (a) Image and (b) classification map of Cerro Cora National Park.

and after the fire, but also from the past to the present. In addition, the region must have a climate without severe cloudiness when the images are taken. Finally, analysis data, such as forest maps or vegetation distributions in the relevant area, should be readily available. Cerro Cora National Park is an area that satisfies all of the above conditions and is thus suitable for this study's purpose. Furthermore, this area is ecologically important because it is composed of districts with distinct vegetation so that the wildfire impact on each zone can be demonstrated.

Figure 4 shows the image and classification maps of Cerro Cora National Park. Through the boundary, it is possible to determine the total damage size and changes in characteristics. The results of the site are of great significance because they can be utilized for prevention, preparedness, response, and recovery in not only Cerro Cora National Park, but also other national parks, as they are the results of considering regional characteristics.

3. Results and Discussion

3.1 Long-term analysis

3.1.1 Wildfire impact and recovery in overall area

The change and repetition of the vegetation index depending on the season have already been proven through previous studies,[24,30] as shown in Fig. 5. However, because this study was conducted with awareness of the research results of Clark *et al.*, the data acquisition cycle is longer than in the previous study. The longer data acquisition cycle of this study does not distort the results because the data were acquired when the vegetation index is the highest and the lowest, and there are no rapid changes. In particular, because significant vegetation changes do not occur during the months around the data acquisition dates,[30] the collected data are valid as samples to analyze long-term seasonal trends. This can also be seen from the August 2020 Landsat data. Changes in Landsat's NBR and NDVI appear to be negligible during this period.

From this perspective, wildfires cause rapid declines in NBR and NDVI in a short period of time, which differ from past seasonal trends. This is evident in the Landsat and Sentinel data. As for the decline, the NDVI calculated from Sentinel is the smallest and the NBR calculated from Sentinel is the largest.

On the basis of long-term data, it is possible to determine the degree of restoration of vegetation damage. According to the NBR and NDVI data obtained from Landsat, it can be seen that the NBR and NDVI have recovered to a level similar to that at the same time in previous years after January 2022. However, the data obtained from Sentinel show a different result. The NBR and NDVI acquired from Sentinel after January 2022 are much lower than those for the same period in previous years. The spectral wavelengths of the Landsat and Sentinel images used to obtain the NBR and NDVI are similar but yield different results. Therefore, it is judged

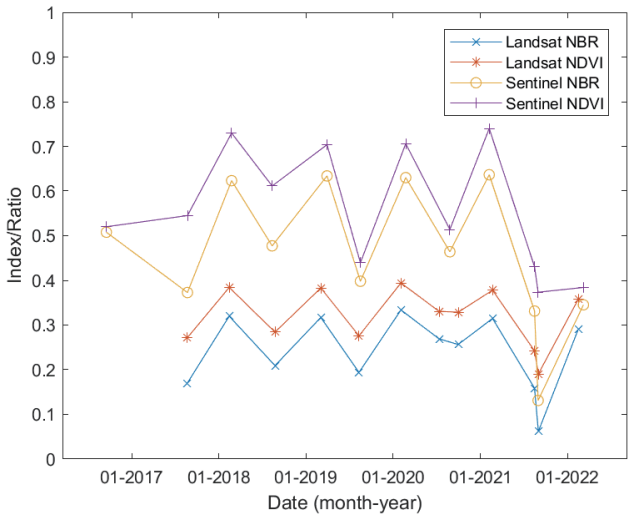

Fig. 5. (Color online) NBR and NDVI trends in Cerro Cora National Park within five years.

that calibration is necessary for a quantitative analysis of the recovery from wildfires in the region.

3.1.2 Wildfire impact and recovery in section

Figure 6 shows the NBR and NDVI of each region of Cerro Cora National Park. It can be seen that the NBR and NDVI trends of each region have similar results with no significant difference from the overall regional trends. The least damaged area is Grassland. In this area, NBR and NDVI were lower than those in other areas, and it can be seen that the damage caused by forest fire is much less. Nevertheless, it can be seen that the indicators of Grassland in February 2022 were lower than those in previous years. Although the direct damage from the wildfire was very small, it is likely that this region was indirectly affected by related factors, such as a decrease in soil moisture content. In contrast, Cerrado, one of the savanna areas similar to Cerradon, displays an opposite trend to Grassland. Although the area suffered rapid damage due to the wildfire, it is rapidly recovering to a level similar to that of the previous year.

In the NBR [Fig. 6(a)] and NDVI [Fig. 6(b)] obtained from Landsat, there is a difference in the amount of change by period and region, but the overall trend is fairly uniform. In contrast,

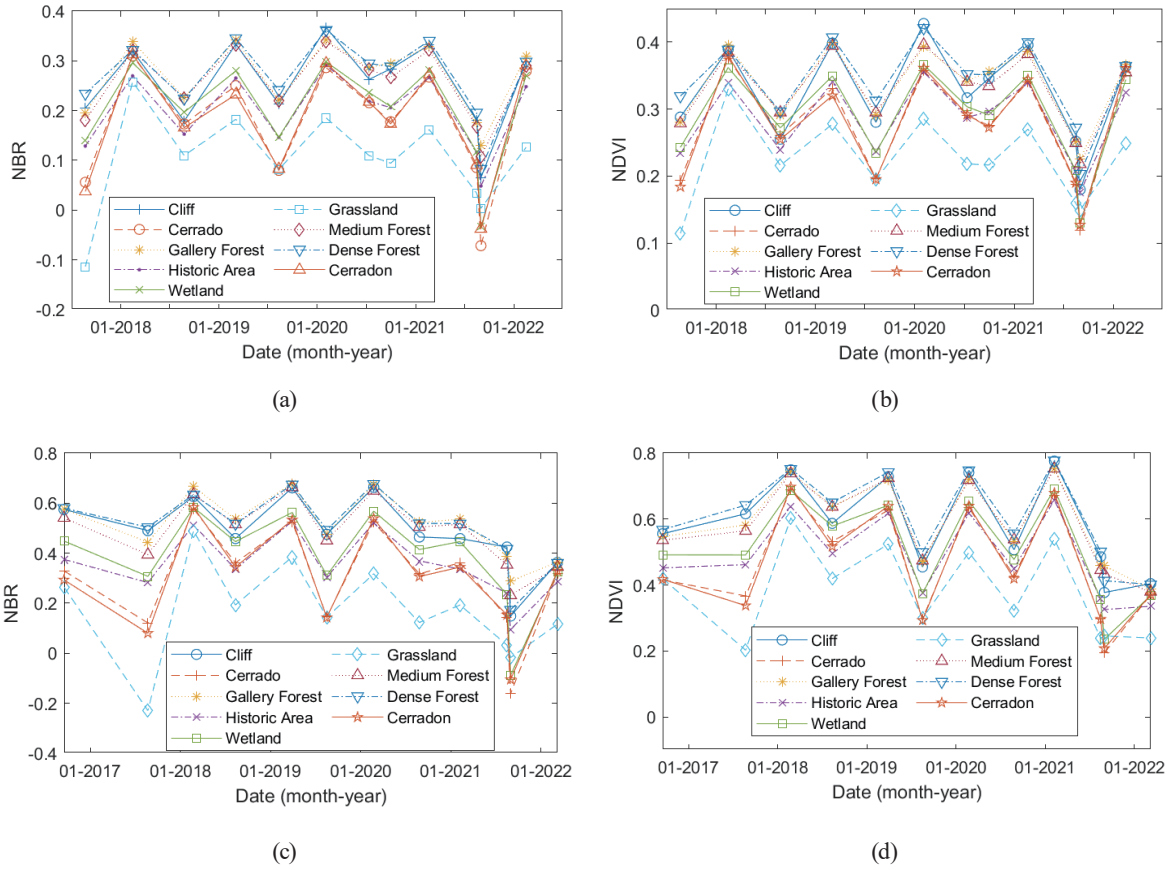

Fig. 6. (Color online) Indices versus date by section from (a) NBR in Landsat, (b) NDVI in Landsat, (c) NBR in Sentinel, and (d) NDVI in Sentinel.

the NBR [Fig. 6(c)] and NDVI [Fig. 6(d)] obtained from Sentinel show different trends for each region. The Sentinel NBR data acquired between August 2020 and March 2021 illustrate this well. Overall, NBR increased, but those of Historic Area, Dense Forest, and Cliff decreased. Similarly, according to the NDVI obtained from Sentinel around March 2022, vegetation restoration in Historic Area is negligible, and the Grassland and Dense Forest regions were not restored. It can be seen that the difference between the real surface and the satellite image is significant despite the data from a similar period. This suggests that studies that compare and correct different satellite images are needed to improve the accuracy of future analyses.

3.2 Short-term analysis

3.2.1 Wildfire severity assessment

As shown in Fig. 6, there are differences between NBR and NDVI in the Landsat and Sentinel images for each region, but the overall trends are similar. The severity of forest fire can be inferred from short-term differences in indicators immediately before and after the fire. In this study, according to a previous study by Keeley,[10] the differential NBR (dNBR) and NDVI (dNDVI) were calculated to identify the severity of forest fire.

Figure 7 shows the differences and severity of each section by indices and images. In general, dNDVI tends to be less than dNBR, and the index differences obtained from Sentinel tend to be larger than those from Landsat. Because Keeley focused on dNBR, the results cannot be applied to dNDVI. Furthermore, that study used Landsat images and has limited applicability to Sentinel images. However, on the basis of the dNBR of the Landsat image, according to the previous study, four of the nine areas can be considered unburned, and the remaining five areas can be considered to show low severity; this appears to underestimate the damage from the forest fire (Table 4). In contrast, the damage according to the dNBR of the Sentinel image was greater than that measured using the Landsat image.

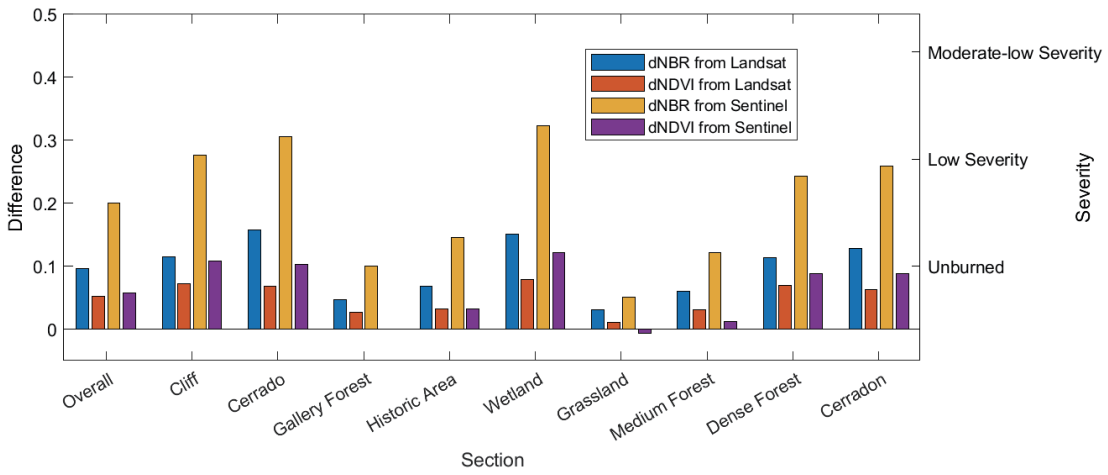

Fig. 7. (Color online) Differences and severity of each section by indices and images.

Table 4
dNBR, dNDVI, and severity from Landsat and Sentinel images by section.

	Landsat			Sentinel		
	dNBR	dNDVI	Severity	dNBR	dNDVI	Severity
Overall	0.0966	0.0516	Unburned	0.2001	0.0569	Low Severity
Cliff	0.1148	0.0720	Low Severity	0.2760	0.1085	Moderate-low
Cerrado	0.1569	0.0684	Low Severity	0.3055	0.1032	Moderate-low
Gallery Forest	0.0464	0.0261	Unburned	0.0998	−0.0004	Unburned
Historic Area	0.0679	0.0319	Unburned	0.1455	0.0321	Low Severity
Wetland	0.1502	0.0784	Low Severity	0.3227	0.1216	Moderate-low
Grassland	0.0303	0.0105	Unburned	0.0501	−0.0063	Unburned
Medium Forest	0.0606	0.0312	Unburned	0.1221	0.0117	Low Severity
Dense Forest	0.1132	0.0688	Low Severity	0.2432	0.0879	Low Severity
Cerradon	0.1282	0.0632	Low Severity	0.2585	0.0887	Low Severity

3.2.2 Damaged area assessment

The area damaged by forest fire was calculated in two ways. The first method is simply to measure the area where NDVI and NBR degradation occurred. The NDVI and NBR declined slightly in the period during the fire owing to seasonal effects. To correct this, the decrease in the index due to seasonal effects was determined in areas undamaged by the fire in order to remove the seasonal effects and identify the decrease in the index due to the forest fire. After this correction, the area of the region where NDVI and NBR degradation occurred was calculated. The second method is to obtain the area for each severity level through dNBR. In this method, the severity can be calculated from the dNBR obtained from the Landsat and Sentinel images, and the areas for each severity and each section are calculated according to the severity.

Figure 8 shows the area damaged by the fire in Cerro Cora National Park using Landsat images as the first method, and Table 5 shows the area and ratio of the damage. It can be seen that the damaged areas calculated using NBR and NDVI are not significantly different. In the lower and upper left corners of Cerro Cora National Park, the damage caused by the wildfire is clearly identified. However, in the central area and right side of the park, non-agglomerated dot-shaped areas are widely distributed. Thus, it is necessary to clarify whether this area is an actual fire-damaged area or simply noise by performing field investigation.

Although there is a slight difference in damaged area calculated with NBR and NDVI, the trend is basically the same. It is estimated that more than 37 km^2 of the park's total area of 57 km^2 was damaged (over 65%). The most affected area in the Cerro Cora area is the Dense Forest, which suffered more than 13 km^2 of damage, and the least affected area was Grassland, with less than 0.3 km^2 of damage. In terms of percentage, Wetland suffered more than 90% damage, whereas Grassland suffered less than 50%.

Figure 9 and Table 6 demonstrate the estimation of the area damaged by the fire using Sentinel images. From the Sentinel images, the difference between estimating the damaged area with NBR and that with NDVI is very large compared with that from Landsat images. The damaged area estimated using NBR from the Sentinel images is similar to that estimated using the Landsat images, but smaller. In contrast, the damaged area calculated using NDVI from the

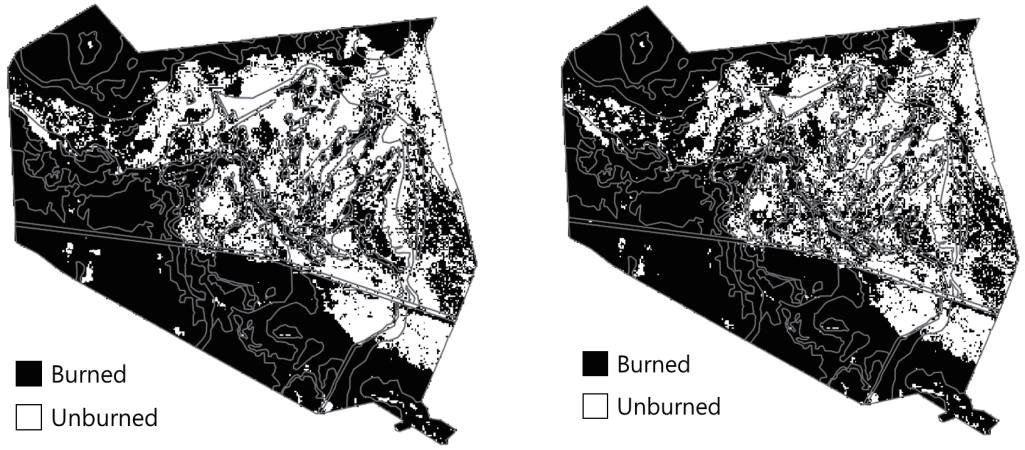

(a) (b)

Fig. 8. Damaged area estimation using (a) NBR and (b) NDVI from Landsat images.

Table 5
Damaged area estimation using Landsat images.

	Area (km^2)	NBR		NDVI	
		Damaged area (km^2)	Damage rate (%)	Damaged area (km^2)	Damage rate (%)
Overall	56.8124	37.9062	66.7216	39.1059	68.8333
Cliff	1.8633	1.5381	82.5471	1.5354	82.4022
Cerrado	9.7163	8.3322	85.7550	8.1090	83.4578
Gallery Forest	9.3983	4.4964	47.8427	5.1480	54.7759
Historic Area	1.3064	0.7650	58.5577	0.7713	59.0400
Wetland	0.6945	0.6570	94.6036	0.6453	92.9189
Grassland	0.6032	0.2583	42.8197	0.2898	48.0416
Medium Forest	13.0989	7.1208	54.3619	7.6059	58.0652
Dense Forest	18.1525	13.0842	72.0792	13.4352	74.0128
Cerradon	1.9790	1.6542	83.5860	1.5660	79.1293

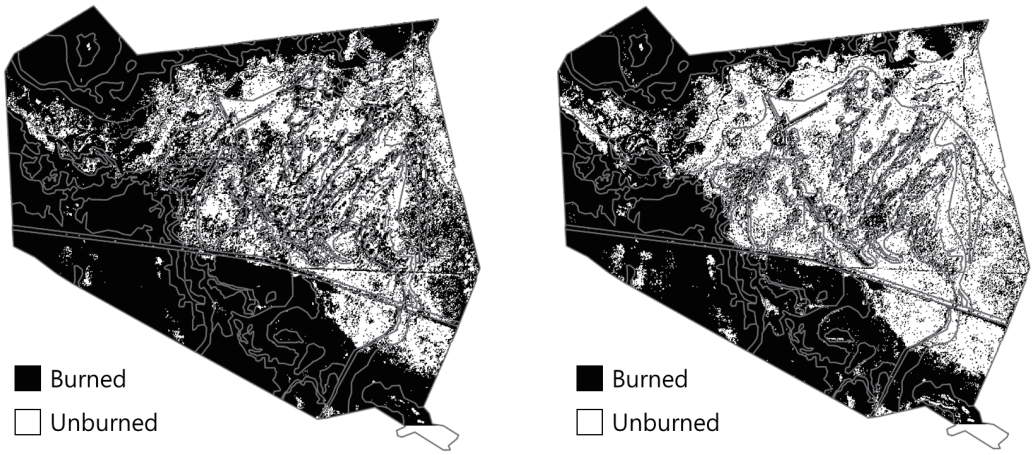

(a) (b)

Fig. 9. Damaged area estimation using (a) NBR and (b) NDVI from Sentinel images.

Table 6
Damaged area estimation using Sentinel images.

	Area (km^2)	NBR		NDVI	
		Damaged area (km^2)	Damage rate (%)	Damaged area (km^2)	Damage rate (%)
Overall	56.8124	39.0438	68.7240	32.2206	56.7140
Cliff	1.8633	1.3123	70.4288	1.0633	57.0654
Cerrado	9.7163	8.0846	83.2067	7.7637	79.9040
Gallery Forest	9.3983	5.3932	57.3849	3.6377	38.7059
Historic Area	1.3064	0.8779	67.1998	0.7599	58.1673
Wetland	0.6945	0.6471	93.1781	0.5493	79.0955
Grassland	0.6032	0.2751	45.6047	0.3182	52.7496
Medium Forest	13.0989	7.3957	56.4605	5.3309	40.6973
Dense Forest	18.1525	13.5075	74.4111	11.3184	62.3516
Cerradon	1.9790	1.5504	78.3410	1.4792	74.7433

Sentinel images was evaluated to be relatively small. Similar to that from the Landsat images, the damaged area calculated from the Sentinel images is about 40 km^2, and the proportion is about 70%. The area obtained from NDVI is about 32 km^2, accounting for 56% of the total area. The trend is similar for all other regions. Therefore, as a result of calculating the damaged area through Landsat and Sentinel images using NBR and NDVI, at least 32 km^2 (55%) was found to be damaged by the wildfire.

When the damaged area is calculated using the dNBR obtained from both Landsat and Sentinel images by Keeley's method,[10] the results shown in Fig. 10 and Tables 7 and 8 can be derived. In the case of classification using the dNBR obtained from Landsat images, the damage appears to be small. This can be understood by comparing Fig. 10(a) with Fig. 8(a). The damage patterns of the lower and upper left areas of the national park are the same, but the damage intensity appears to be low [Fig. 10(a)]. In contrast, the area where no damage occurred appears to be distributed over a wider range. As indicated in Table 7, the area where fire does not appear to have occurred out of the total area is about 35 km^2 or more. From Table 5, it can be seen that the damaged area is small and the damage intensity is low, and the area without damage is less than about 20 km^2. Similarly, for classification by dNBR obtained from Sentinel images, the damaged area is smaller, as shown by comparing Tables 6 and 8. It can be seen that this applies not only to the entire national park, but also to the individual regions within it.

However, it can be seen that the measured damage intensity is higher than that of Landsat. This is consistent with the trend observed in Fig. 7. The trends shown in Figs. 10 and Figs. 7 are similar for the amount of damage obtained from the Sentinel and Landsat images. Therefore, the damaged area, measured considering only the change in NBR, is larger than the area measured based on severity, but the damage intensity and tendency are similar.

3.2.3 Land characteristic variation

In addition to changes in vegetation index, the wildfire changes the characteristics of the area. The tasseled cap transformation enables the changes in the properties of a region to be interpreted using brightness, greenness, and wetness. Figure 11 shows the correlation between

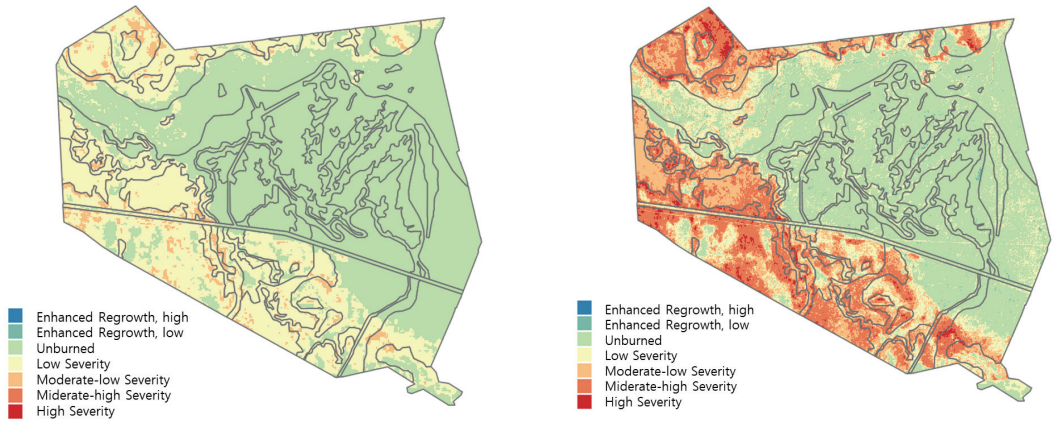

(a) (b)

Fig. 10. (Color online) Damaged area classification using NBR from (a) Landsat and (b) Sentinel images.

Table 7
Damaged area classification using dNBR from Landsat images.

	Enhanced regrowth, high	Enhanced regrowth, low	Unburned	Low severity	Moderate-low severity	Moderate-high severity	High severity
Overall	0.0000	0.0000	35.1234	19.5066	2.1573	0.0000	0.0000
Cliff	0.0000	0.0000	0.9648	0.7758	0.1233	0.0000	0.0000
Cerrado	0.0000	0.0000	3.3534	5.9157	0.4518	0.0000	0.0000
Gallery Forest	0.0000	0.0000	8.1468	1.2033	0.0423	0.0000	0.0000
Historic Area	0.0000	0.0000	0.9918	0.2817	0.0225	0.0000	0.0000
Wetland	0.0000	0.0000	0.2367	0.3834	0.0783	0.0000	0.0000
Grassland	0.0000	0.0000	0.6093	0.0000	0.0000	0.0000	0.0000
Medium Forest	0.0000	0.0000	10.4157	2.4624	0.2205	0.0000	0.0000
Dense Forest	0.0000	0.0000	9.4815	7.4889	1.1538	0.0000	0.0000
Cerradon	0.0000	0.0000	0.9234	0.9954	0.0648	0.0000	0.0000

Table 8
Damaged area classification using dNBR from Sentinel images.

	Enhanced regrowth, high	Enhanced regrowth, low	Unburned	Low severity	Moderate-low severity	Moderate-high severity	High severity
Overall	0.0030	0.2455	27.7354	9.0082	9.3058	9.3510	0.8183
Cliff	0.0000	0.0041	0.4652	0.3240	0.3420	0.3692	0.0430
Cerrado	0.0000	0.0087	2.9062	0.6579	3.0950	2.9775	0.0660
Gallery Forest	0.0030	0.0680	6.0783	2.2967	0.6750	0.2592	0.0130
Historic Area	0.0000	0.0118	0.6964	0.3499	0.1165	0.1195	0.0116
Wetland	0.0000	0.0000	0.1457	0.1216	0.2310	0.1622	0.0338
Grassland	0.0000	0.0001	0.5536	0.0492	0.0000	0.0000	0.0000
Medium Forest	0.0000	0.1027	8.8133	1.8214	1.2094	1.0454	0.0959
Dense Forest	0.0000	0.0490	7.2717	3.2598	3.0296	3.9966	0.5392
Cerradon	0.0000	0.0011	0.8050	0.1277	0.6073	0.4214	0.0158

elements of brightness, greenness, and wetness of each section from Landsat images before and after the fire. Figure 12 shows the statistical distributions of the brightness, greenness, and wetness of each zone from Landsat images.

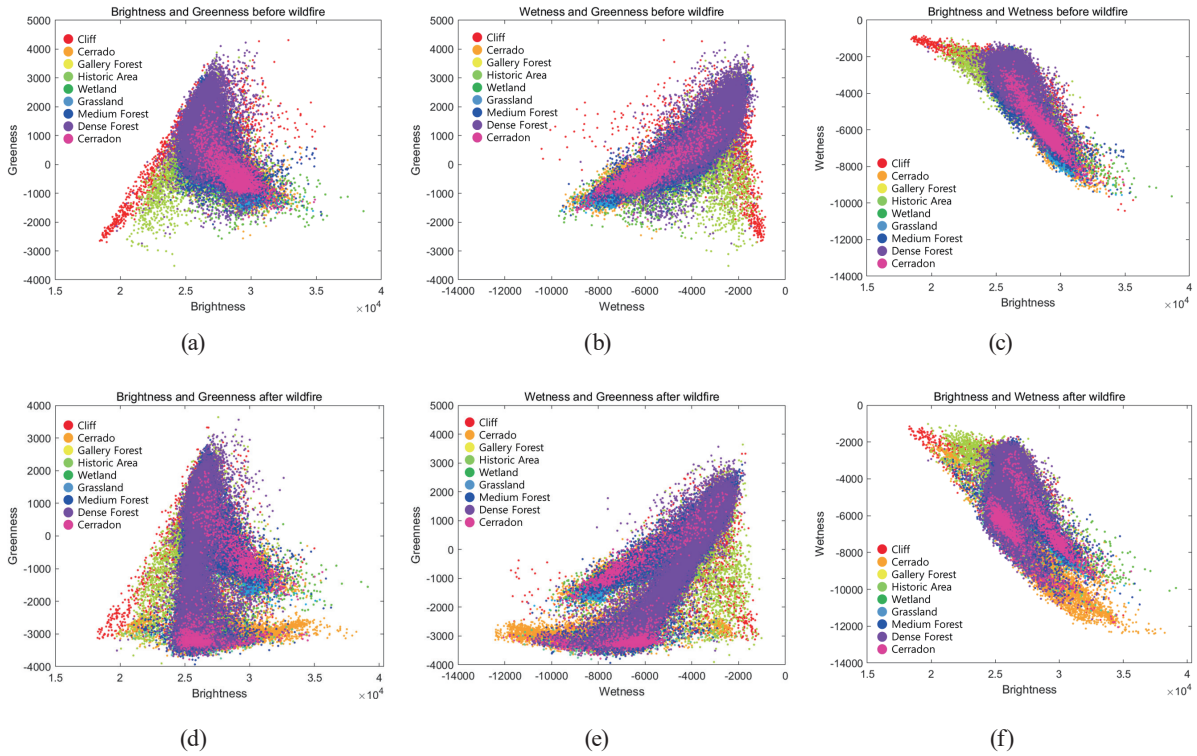

Fig. 11. (Color online) Tasseled cap planes from Landsat images: (a) brightness and greenness, (b) wetness and greenness, (c) brightness and wetness before wildfire, (d) brightness and greenness, (e) wetness and greenness, and (f) brightness and wetness after wildfire.

In the overall trend from Landsat images, it is observed that the change in brightness before and after the wildfire is not significant, but the greenness and wetness tend to decrease. Therefore, the damage caused by the forest fire did not significantly affect the reflectivity of the area. However, the damage to the vegetation and the moisture content were reduced.

Figure 11 shows the changes in land characteristics and the differences between areas before and after the fire. In particular, compared with Figs. 11(a)–11(c), Figs. 11(d)–11(f) show a tendency of the land characteristics to be distributed into two clusters rather than be densely concentrated. As one cluster was dispersed into two clusters, the dispersed cluster moved in the direction of decreasing wetness and greenness. In other words, it can be seen that there are no changes in the characteristics of areas without damage, whereas decreases in vegetation and moisture content occurred in areas damaged by the fire.

Figure 12 shows the specific characteristic change for each area. As can be seen in Fig. 12(a), there is no significant change in brightness for each area, except for the Cerradon region. In contrast, in Fig. 12(b), it can be seen that greenness significantly decreased in all areas except for Gallery Forest and Grassland. This indicates that overall vegetation damage occurred in all areas except for two areas. It can be seen that the moisture content of each area decreased as a whole.

The results analyzed using Sentinel images are different from those analyzed using Landsat images. Figure 13 shows the land characteristics obtained from the tasseled cap transformation

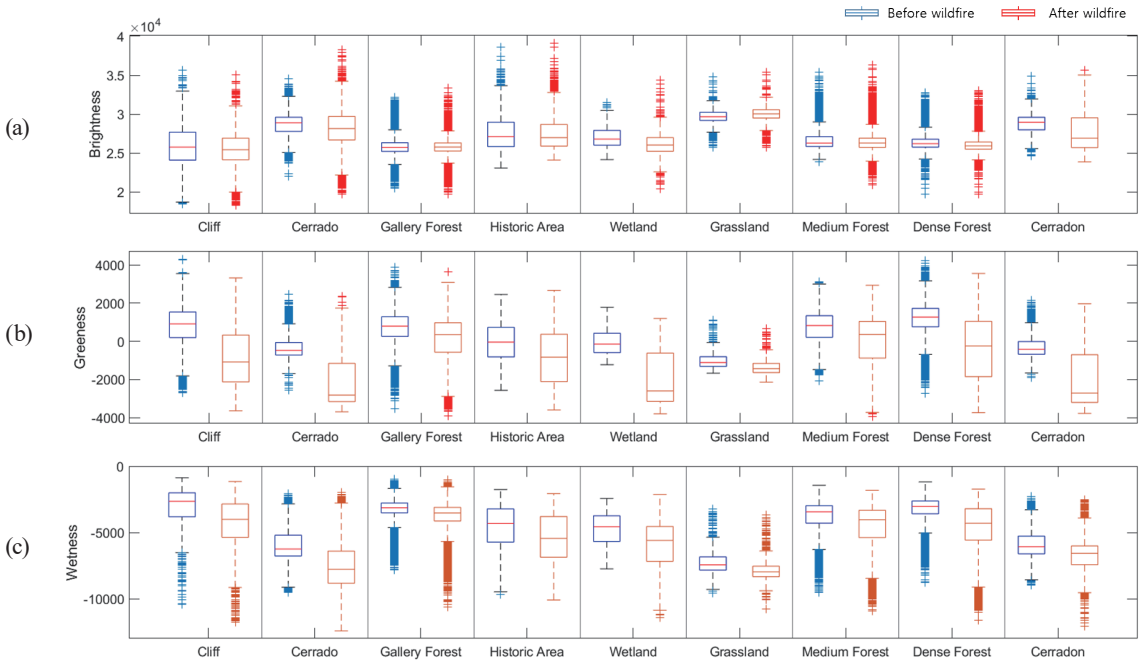

Fig. 12. (Color online) Box plots of (a) brightness, (b) greenness, and (c) wetness of each section from Landsat images before and after wildfire.

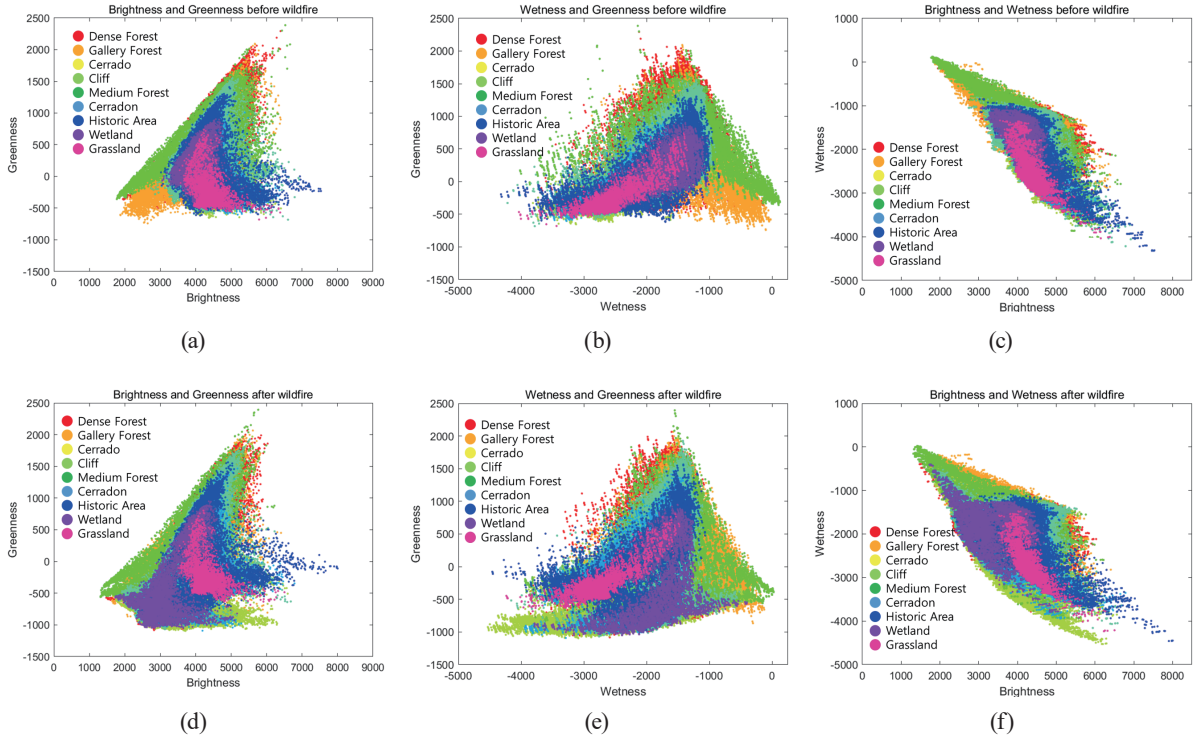

Fig. 13. (Color online) Tasseled cap planes from Sentinel images: (a) brightness and greenness, (b) wetness and greenness, (c) brightness and wetness before wildfire, (d) brightness and greenness, (e) wetness and greenness, and (f) brightness and wetness after wildfire.

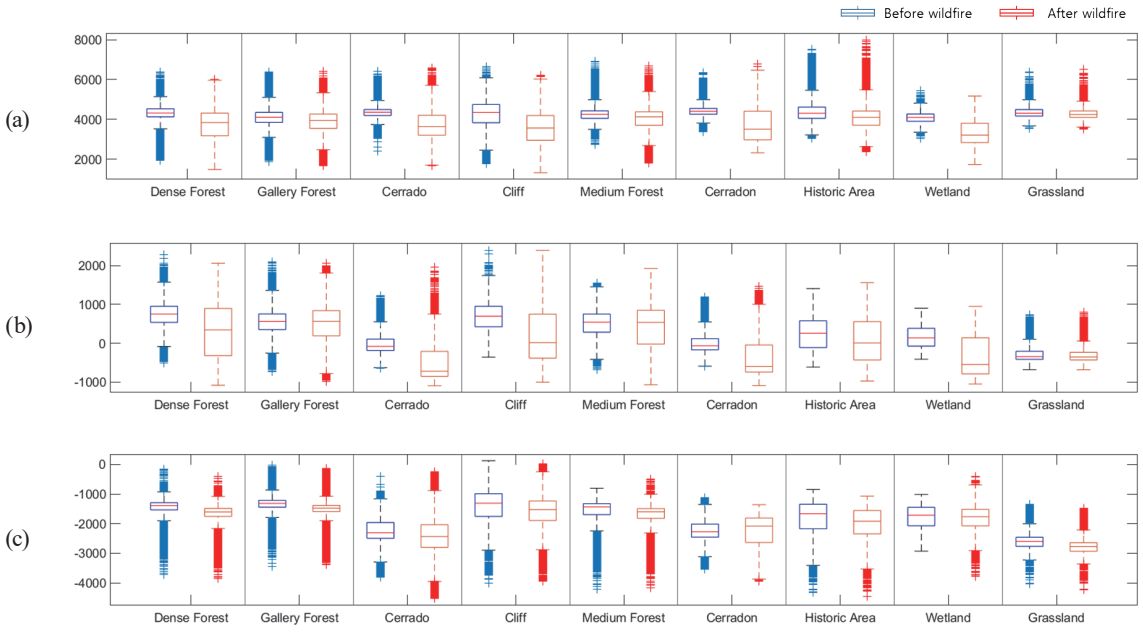

Fig. 14. (Color online) Box plots of (a) brightness, (b) greenness, and (c) wetness of each section from Sentinel images before and after wildfire.

using Sentinel images. A decrease in greenness occurs after the forest fire, as in the analysis result obtained using Landsat images. However, unlike the Landsat images, where there is little change in brightness, the brightness obtained through Sentinel images showed a large change.

It can be seen that brightness considerably decreased in large areas damaged by the fire, such as Dense Forest, Cerrado, Cerradon, and Wetland (Fig. 14). This indicates that the forest fire not only destroyed the vegetation and reduced the moisture content, but also lowered the reflectivity. The observed decrease in reflectance, which could not be measured from the Landsat images, suggests that the wildfire in Cerro Cora National Park has a certain impact on global warming by destroying the vegetation and generating CO_2, as well as by reducing the albedo.

The variations in greenness and wetness are similar in both the Landsat and Sentinel cases. This proves that the results obtained from both types of images are reliable. Therefore, there is no doubt that the wildfire in Cerro Cora National Park caused vegetation damage and water content loss in the areas studied.

4. Conclusions

In this study, we analyzed the impact of the wildfire that occurred in Cerro Cora National Park. NDVI and NBR were obtained from Landsat and Sentinel images to understand the effects of the forest fire from a long-term perspective, and the damaged area and its severity were estimated. In addition, by using the tasseled cap transformation, changes in the characteristics of each area were identified.

This study has several limitations. The first is that the image acquisition times of Landsat and Sentinel do not exactly coincide. This may cause small errors, which may affect the results.

Second, the satellite images were limited to Landsat and Sentinel, and only NDVI and NBR were compared. If various image platforms such as KOMPSAT and MODIS are used or if various indicators such as ratio vegetation index (RVI) and enhanced vegetation index (EVI) are applied, different results may be obtained. These factors should be addressed in future research. Likewise, the result of the brightness aspect of the tasseled cap transformation is also different between Landsat and Sentinel images. This may be because of the coefficient or other factors. To determine the exact factors that cause these differences, a further study focused on the coefficient varying with the test area is needed.

Nevertheless, the significance of this study is as follows. First, from a long-term perspective, the effects of the wildfire in Cerro Cora National Park on seasonal vegetation changes were investigated. Because Cerro Cora National Park is vast, it is difficult to verify its status and determine the damage accurately because of limited access. In addition, owing to the periodic resolution of satellite images, seasonal factors are reflected, making it difficult to determine the damage solely due to fire. In this study, it is meaningful that the forest fire damage was calculated considering seasonal effects based on previous research cases and actual data. In addition, analysis was performed on the restoration of fire-damaged areas based on seasonal trends. These methodologies and results are of great significance because they can be used to calculate the damage of forest fire in other regions in the future.

Second, the severity of damage to each section of the national park was evaluated, and the damaged area was estimated on the basis of severity. As mentioned in the introduction, it is very important to understand the severity of the fire as well as the area. Not only was the damaged area calculated, but also a severity map was produced. These are essential data for policymaking and research on forest fire prevention, preparedness, response, and recovery. Therefore, this study is significant in that it produced important data for subsequent research in this field.

Third, changes in land characteristics due to fire were identified for each section. In addition to the area and intensity of damage, changes in the characteristics of the area were identified. Each area of the national park is closely related not only to the change in vegetation, but also to the ecosystem of the area and, furthermore, to the global environment. Through this study, it was identified that forest fire in the area not only increased the amount of carbon dioxide and reduced the amount of oxygen produced by simply destroying vegetation, but also negatively affected global warming by lowering the water content and albedo in the region. This has important implications not only for research on forests and vegetation, but also for global atmospheric science and environmental science in general. From this perspective, this study has great significance in that it is closely related to global environmental issues.

Finally, previous studies and analysis methodologies were compared to determine the impact of wildfires. There are many precedent studies to understand the effects of wildfires. In this study, an appropriate methodology was presented from among those in previous studies, and research results were derived by applying the methodology. The results obtained using Landsat and Sentinel images, as well as those obtained using NBR and NDVI, were compared. This not only improves the reliability of the results compared with those obtained by applying a single method, but also compares and analyzes the characteristics, advantages, and disadvantages of each method. Therefore, the results can be used to select an appropriate method for further research. The results of this study go beyond the scope of simply estimating wildfire damage and can be used as comparative data between methods for investigating wildfire damage.

The results of this study, obtained by analyzing the effects of the wildfire in Cerro Cora National Park from various perspectives, can be used as data for forest fire, remote sensing, and global environment-related research.

References

1 J. J. W. Rouse, R. H. Haas, J. A. Schell, and D. W. Deering: Monitoring Vegetation Systems in the Great Plains with Erts, https://ntrs.nasa.gov/api/citations/19730017588/downloads/19730017588.pdf (accessed August 2022).
2 L. Collins, G. McCarthy, A. Mellor, G. Newell, and L. Smith: Remote Sens. Environ. **245** (2020) 111839. https://doi.org/10.1016/j.rse.2020.111839
3 S. T. Seydi, M. Akhoondzadeh, M. Amani, and S. Mahdavi: Remote Sens. **13** (2021) 220. https://doi.org/10.3390/rs13020220
4 S.-M. Lee and J.-C. Jeong: Korean J. Remote Sens. **35** (2019) 10 (in Korean). https://doi.org/10.7780/kjrs.2019.35.6.4.4
5 S.-J. Lee and Y.-W. Lee: Korean J. Remote Sens. **36** (2020) 11 (in Korean). https://doi.org/10.7780/kjrs.2020.36.1.3
6 F. J. Kriegler, W. A. Malila, R. F. Nalepka, and W. Richardson: Remote Sens. Environ. VI (1969) 97. https://ui.adsabs.harvard.edu/abs/1969rse..conf...97K (accessed August 2022).
7 D. Bafi: Proc. SafeGreece 2020 on-line (2020) 55.
8 A. Gemitzi and N. Koutsias: Remote Sens. Appl.: Soc. Environ. **26** (2022) 100720. https://doi.org/10.1016/r.rsase.2022.100720
9 S. Hislop, S. Jones, M. Soto-Berelov, A. Skidmore, A. Haywood, and T. H. Nguyen: Remote Sens. **10** (2018) 460. https://doi.org/10.3310/rs10030460
10 J. E. Keeley: Int. J. Wildland Fire **18** (2009) 116. https://doi.org/10.1071/wf07049
11 P. R. Robichaud, S. A. Lewis, R. E. Brown, E. D. Bone, and E. S. Brooks: Hydrol. Process. **34** (2020) 4431. https://doi.org/10.1002/hyp.13882
12 Y. Sánchez Sánchez, A. Martínez Graña, and F. Santos-Francés: Agronomy **11** (2021) 1459. https://doi.org/10.3390/agronomy11081459
13 F. Serra-Burriel, P. Delicado, A. T. Prata, and F. M. Cucchietti: Remote Sens. Environ. **265** (2021) 112649. https://doi.org/10.1016/j.rse.2021.112649
14 A. Wibowo: bioRxiv (2022). https://doi.org/10.1101/2022.01.29.478296 (accessed August 2022).
15 D. Chen, C. Fu, J. V. Hall, E. E. Hoy, and T. V. Loboda: Remote Sens. Environ. **258** (2021) 112393. https://doi.org/10.1016/j.rse.2021.112393
16 X. Huang: Univ. Br. Columbia Lib. (2021). https://doi.org/10.14288/1.0396742 (accessed August 2022).
17 R. F. Kokaly, B. W. Rockwell, S. L. Haire, and T. V. V. King: Remote Sens. Environ. **106** (2007) 305. https://doi.org/10.1016/j.rse.2006.08.006
18 A. Nolè, A. Rita, M. F. Spatola, and M. Borghetti: Sci. Total Environ. **823** (2022) 153807. https://doi.org/10.1016/j.scitotenv.2022.153807
19 C. W. Smith, S. K. Panda, U. S. Bhatt, F. J. Meyer, A. Badola, and J. L. Hrobak: Remote Sens. **13** (2021) 1966. https://doi.org/10.3390/rs13101966
20 E. P. Crist: Remote Sens. Environ. **17** (1985) 301. https://doi.org/10.1016/0034-4257(85)90102-6
21 P. P. Joshi, R. H. Wynne, and V. A. Thomas: Int. J. Appl. Earth Obs. Geoinf. **82** (2019) 101898. https://doi.org/10.1016/j.jag.2019.101898
22 P. Kacic, A. Hirner, and E. Da Ponte: Remote Sens. **13** (2021) 5105. https://doi.org/10.3390/rs13245105
23 R. J. Kauth and G. Thomas: LARS Symposia (1976) 159. https://citeseerx.ist.psu.edu/viewdoc/download?doi=10.1.1.461.6381&rep=rep1&type=pdf (accessed August 2022).
24 M. A. A. R. Kutubi, M.-G. Hong, S. Hossain, and C. Kim: Proc. 2019 Int. Conf. Electrical, Computer and Communication Engineering (ECCE, 2019) 1. https://doi.org/10.1109/ecace.2019.8679355
25 L. Qingsheng, L. Gaohuan, H. Chong, L. Suhong, and Z. Jun: Proc. 2014 IEEE Geoscience and Remote Sensing Symp. (IGARSS, 2014) 541. https://doi.org/10.1109/igrass.2014.6946479
26 S. M. Ali and S. S. Salman: Al-Sadeq Int. Conf. Multidisciplinary in IT and Communication Science and Applications (AIC-MITCSA, 2016) 1. https://doi.org/10.1109/AIC-MITCSA.2016.7759914
27 T. Shi and H. Xu: IEEE J. Sel. Top. Appl. Earth Obs. Remote Sens. **12** (2019) 4038. https://doi.org/10.1109/jstars.2019.2938388
28 S.-I. Kim, D.-S. Ahn, and S.-C. Kim: Korean J. Remote Sens. **37** (2021) 939 (in Korean). https://doi.org/10.7780/kjrs.2021.37.5.1.9
29 B. Marcos, J. Gonçalves, D. Alcaraz-Segura, M. Cunha, and J. P. Honrado: Int. J. Appl. Earth Obs. GeoInf. **78** (2019) 77. https://doi.org/10.1016/j.jag.2018.12.003
30 M. L. Clark, T. M. Aide, H. R. Grau, and G. Riner: Remote Sens. Environ. **114** (2010) 2816. https://doi.org/10.1016/j.rse.2010.07.001